Technical Report

47 pgs

NOTICE

We are pleased to supply this document in response to your request.

The acquisition of technical reports, notes, memorandums, etc., is an active, ongoing program at the Defense Technical Information Center (DTIC) that depends, in part, on the efforts and interests of users and contributors.

Therefore, if you know of the existence of any significant reports, etc., that are not in the DTIC collection, we would appreciate receiving copies or information related to their sources and availability.

The appropriate regulations are Department of Defense Directive 5200.12, DoD Scientific and Technical Information Program; Department of Defense Directive 5200.20, Distribution Statements on Technical Documents (amended by Secretary of Defense Memorandum, 18 Oct 1983, subject: Control of Unclassified Technology with Military Application); Military Standard (MIL-STD) 847-B, Format Requirements for Scientific and Technical Reports Prepared by or for the Department of Defense; Department of Defense 5200.1R, Information Security Program Regulation.

Our Acquisition Section, DTIC-DDAB, will assist in resolving any questions you may have. Telephone numbers of that office are: (202)274-6847, 274-6874 or Autovon 284-6847, 284-6874.

FEBRUARY 1984

★ U.S. Government Printing Office: 1984—461-148/10611

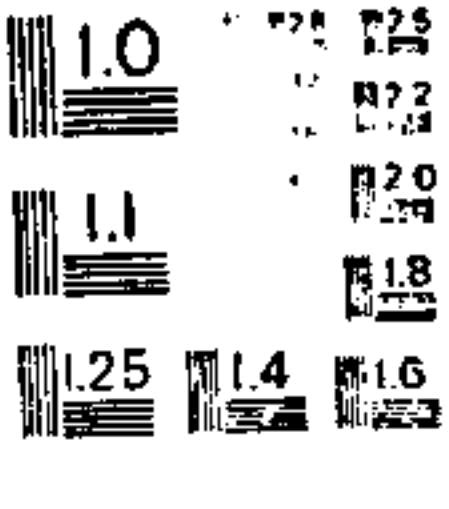

SECURITY MARKING

The classified or limited status of this report applies to each page, unless otherwise marked.
Separate page printouts MUST be marked accordingly.

THIS DOCUMENT CONTAINS INFORMATION AFFECTING THE NATIONAL DEFENSE OF THE UNITED STATES WITHIN THE MEANING OF THE ESPIONAGE LAWS, TITLE 18, U.S.C., SECTIONS 793 AND 794. THE TRANSMISSION OR THE REVELATION OF ITS CONTENTS IN ANY MANNER TO AN UNAUTHORIZED PERSON IS PROHIBITED BY LAW.

NOTICE: When government or other drawings, specifications or other data are used for any purpose other than in connection with a definitely related government procurement operation, the U.S. Government thereby incurs no responsibility, nor any obligation whatsoever; and the fact that the Government may have formulated, furnished, or in any way supplied the said drawings, specifications, or other data is not to be regarded by implication or otherwise as in any manner licensing the holder or any other person or corporation, or conveying any rights or permission to manufacture, use or sell any patented invention that may in any way be related thereto.

EDL-G9DD

UNCLASSIFIED

COPY NO 4 OF 4 COPIES

PROJECT AQUARIUS
QUARTERLY REPORT (U)

BY
R. STANDLEY
K. SNOW

2 MARCH 1970

SPONSORED BY
ADVANCED RESEARCH PROJECTS AGENCY
ARPA ORDER NO. 1459

SYLVANIA
ELECTRONIC DEFENSE LABORATORIES
Mountain View, California

Sylvania Electronic Systems - Western Division
Electronic Defense Laboratories
Mountain View, California

(S) Project AQUARIUS Quarterly Report (U)

Principal Investigator R. Standley 415/966-3731
Project Engineer K. Snow 415/966-3186

ARPA Order No. 1459

Effective Date of Contract: 2 June 1969

Contract Expiration Date: 30 June 1970

Amount of Contract: $118,864

This research was supported by the Advanced Research Projects Agency of the Department of Defense and was monitored by the Office of Naval Research under Contract No. N00014-69-C-0446

(U) TABLE OF CONTENTS (U)

(U) ILLUSTRATIONS (U)

(U) TABLES (U)

SECTION 1.

(U) INTRODUCTION (U)

Project AQUARIUS is a part of the ARPA sponsored ocean surveillance program under Project MAY BELL. The primary goals of Project AQUARIUS are to experimentally demonstrate the feasibility of detecting both submarine launched ballistic missiles and low-flying aircraft and to compare the experimentally observed detection ranges to theoretically predicted detection ranges. The experimental set-up consists of using a bistatic HF continuous wave radar with low power ocean based buoy transmitters and high sensitivity receivers located on the coast. A detection is made by observing the doppler shifted signal that is scattered from moving targets. In this particular experiment the target is illuminated by line-of-sight or ground wave energy from the transmitter. The scattered doppler shifted target return is received by an ionospheric sky-wave as illustrated in Figure 1.

There has been a continuing requirement for this type of long range detection of small targets since a Cuban pilot flying a MIG penetrated the U.S. radar network and was first spotted by the air controller at the Miami airport.

The experimental results of the controlled aircraft tests have been fairly encouraging and indicate that long range aircraft detection is possible using this low power bistatic radar concept. There appears to be a fair agreement between the predicted detection regions and the regions for which the aircraft has been detected. During a total of three controlled aircraft tests, four detections have been made, two of which are detections of the controlled aircraft. However, during one period, that of 18 December, the detected aircraft does not appear to correspond in time or location with

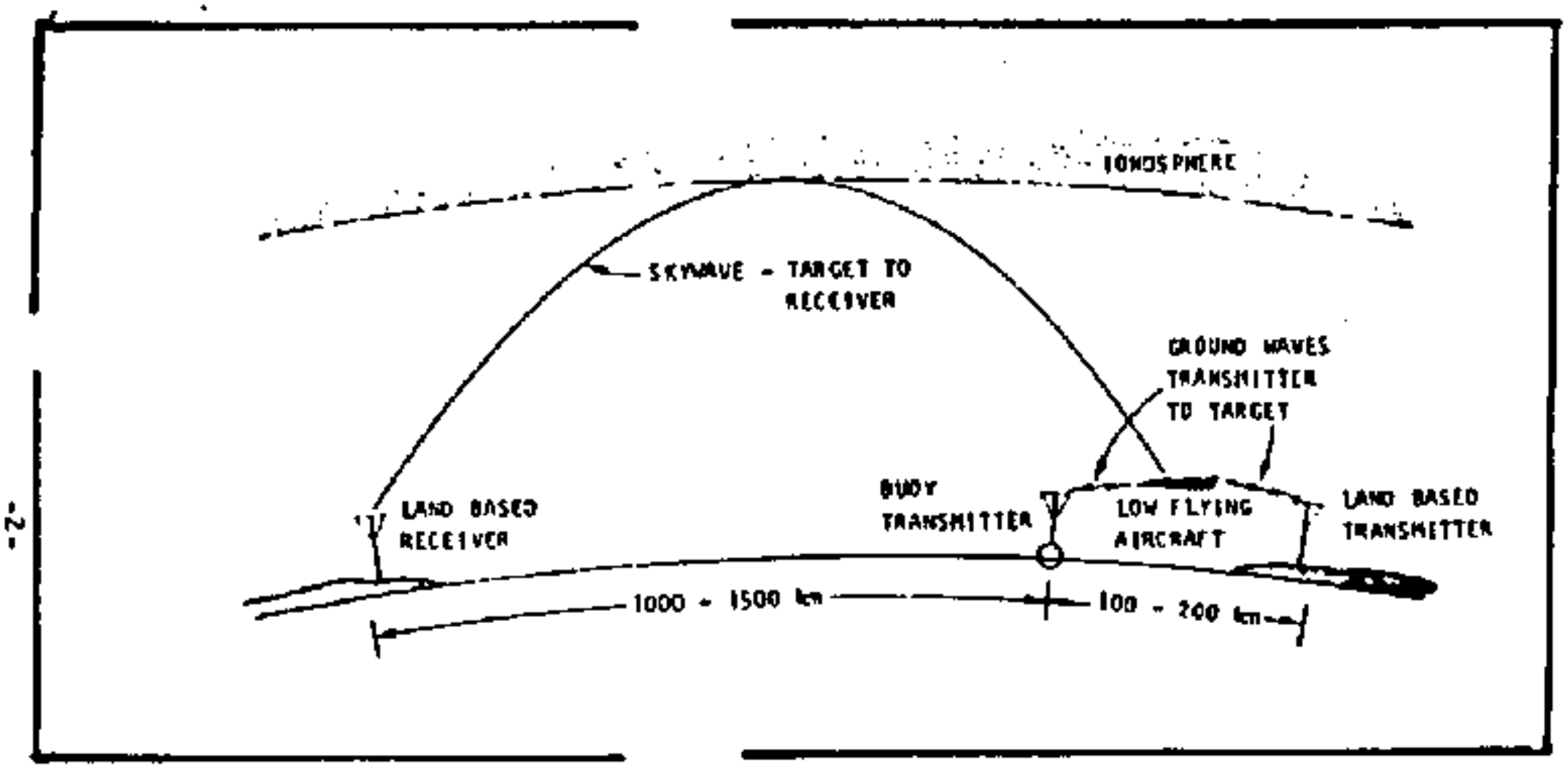

(U)

Figure 1. (S) Illustration of Buoy Tactical Early Warning Concept (U).

UNCLASSIFIED

1.0 (S) (SI) -- Continued.

that of the controlled aircraft. It is surmised that these detections were of an aircraft flying near the receiver rather than the transmitter.

UNCLASSIFIED

1.1 (U) (SI) Repor. Organization.

In Section 2 of this report the basic technique and the hardware being employed for these tests are described. The basic geometry, transmitter and receiver configuration, calibration techniques, propagation calculations, and a description of the propagation program are given in this section. Section 3 contains the description of the detection prediction of Poiseidon launchings from Cape Kenendy using the buoys located approximately 100, 200 and 300 km from the launch area. For that particular geometry and the ranges involved, it is observed that the probability of detecting an SLBM is virtually negligible until the target rises into the ionosphere and acquires a substantially enhanced cross section. Section 4 contains a description of the controlled aircraft tests, flight plans and the detection observations made. Also, in this section is a tabulation of predicted and observed carrier strengths and noise levels. The purpose of these comparisons is to observe with what reliability these parameters can be predicted with the object of accurately predicting system performance. Finally, Section 5 contains a summary of the problems and the basic results obtained to date.

SECRET

UNCLASSIFIED

SECTION 2.

(U) EQUIPMENT AND TECHNIQUES (U)

Due to the nature and the time frame of this project, all of the data collection hardware has been obtained by using equipment developed by other Project MAY BELL participants or by using hardware developed for other programs. Both the buoy and the CW transmitters at Carter Cay used in these tests, are also used for the groundwave measurements which Raytheon is conducting. The receiving system in use belongs to the LSASA field station located at Vint Hill Farms Station, Va. and consists of a linear disposed antenna array and multi-channel HF receiving and recording equipment.

2.1 (U) Transmitter Characteristics.

Two different types of transmitters have been used in the experiment to date. Those tests conducted prior to December used a buoy mounted transmitter of approximately 10 watts radiating at 5.8 and 9.259 Mhz. The antenna on the buoy consists of a top-loaded vertical monopole cut for a quarter wave length at 7.5 Mhz. This buoy was anchored off the coast of Florida approximately 120 kilometers down range and at an azimuth of 113 degrees from Cape Kennedy. The tests conducted in January and February have used the CW transmitters on Carter Cay. The power of these CW transmissions has ranged from 100 watts up to 2.3 kilowatts depending upon time and the particular transmitter in use. All of these transmissions radiate into quarter wave vertical monopoles cut for the frequency in use.

2.2 (U) (S) Receiver Site Characteristics.

Two separate receiving systems have been used at the receiver site located at Vint Hill Farms Station. One receiving system is a van mounted high dynamic range digital processing system containing synthesizer controlled receivers (Sylvania R-27A receivers)*digital spectrum analysis* using a CDC 3700 general purpose computer and both analog and digital PCM recording capability. The second receiver system is located in two back-to-back house trailers, and consists of a DF set connected to an LDAA steerable beam antenna and 12 analog receiving channels using R390A receivers. The R390A receivers connect to both a real time analog spectral display and a 12 channel analog tape recorder. The block diagrams of these two receiving systems are shown in Figures 2 and 3.

2.3 (U) (S) Receiver System Calibration.

One of the more important goals of this project is to be able to predict the detection performance of the buoy tactical early warning system. Thus, it is desired to compare predicted signal and noise values to actual measured data. Then, if there exist significant discrepancies between the actual and observed data, the predictions must be modified to correct this difference.

The standard calibrations that are performed on the system are to measure the received carrier strength and also the received noise power referenced to a 1 Hertz bandwidth. The process of measuring the received carrier strength is a simple procedure of comparing the receiver IF output signal level when it is connected to the antenna, to the IF output level when the receiver is connected to a synthesizer having the same HF frequency as the carrier signal being measured. The average IF output level for that

* Digital Spectrum Analysis not available after January, 1970 due to termination of the computer lease.

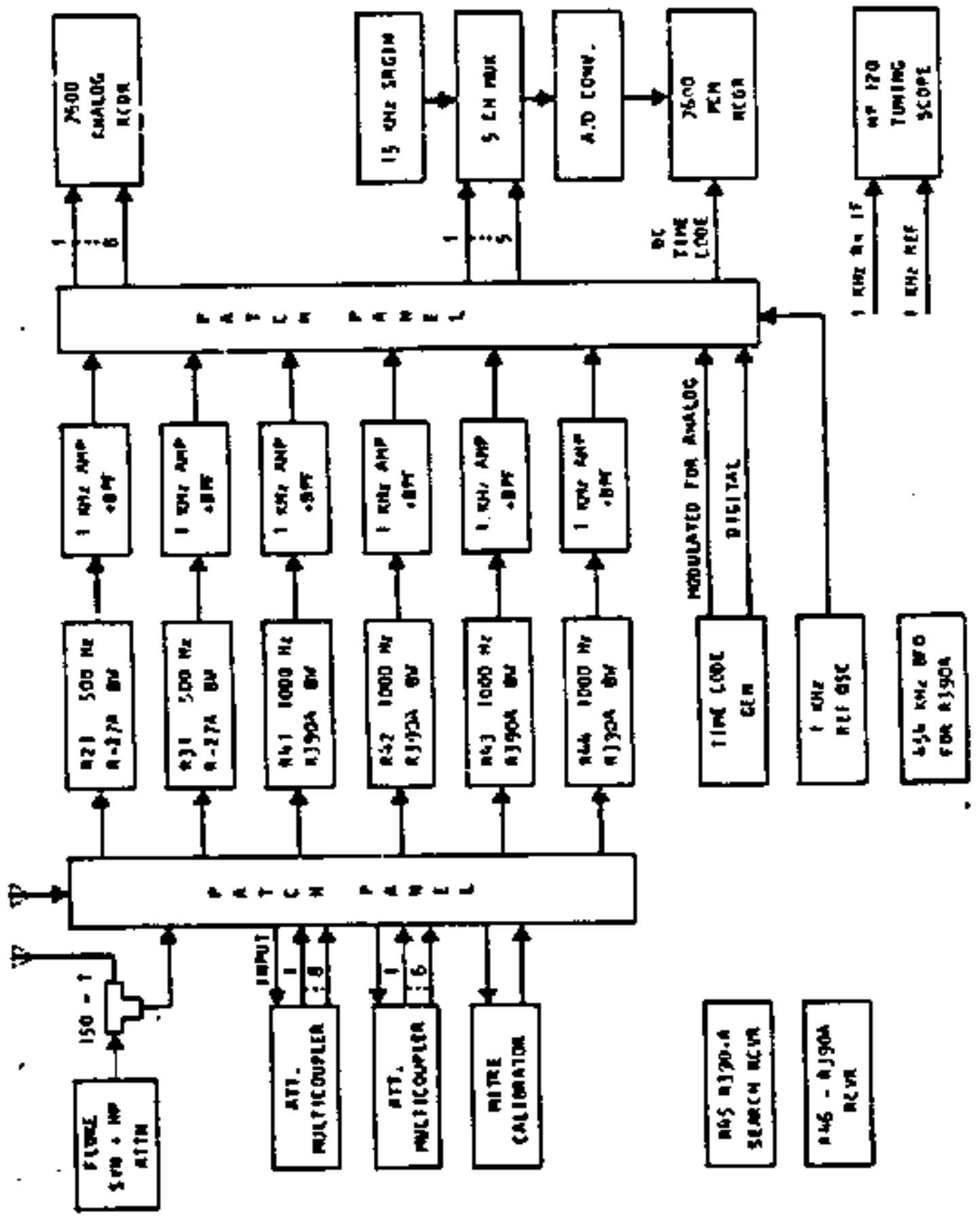

Figure 2. (U) Block Diagram for High Dynamic Range Receiving System (U).

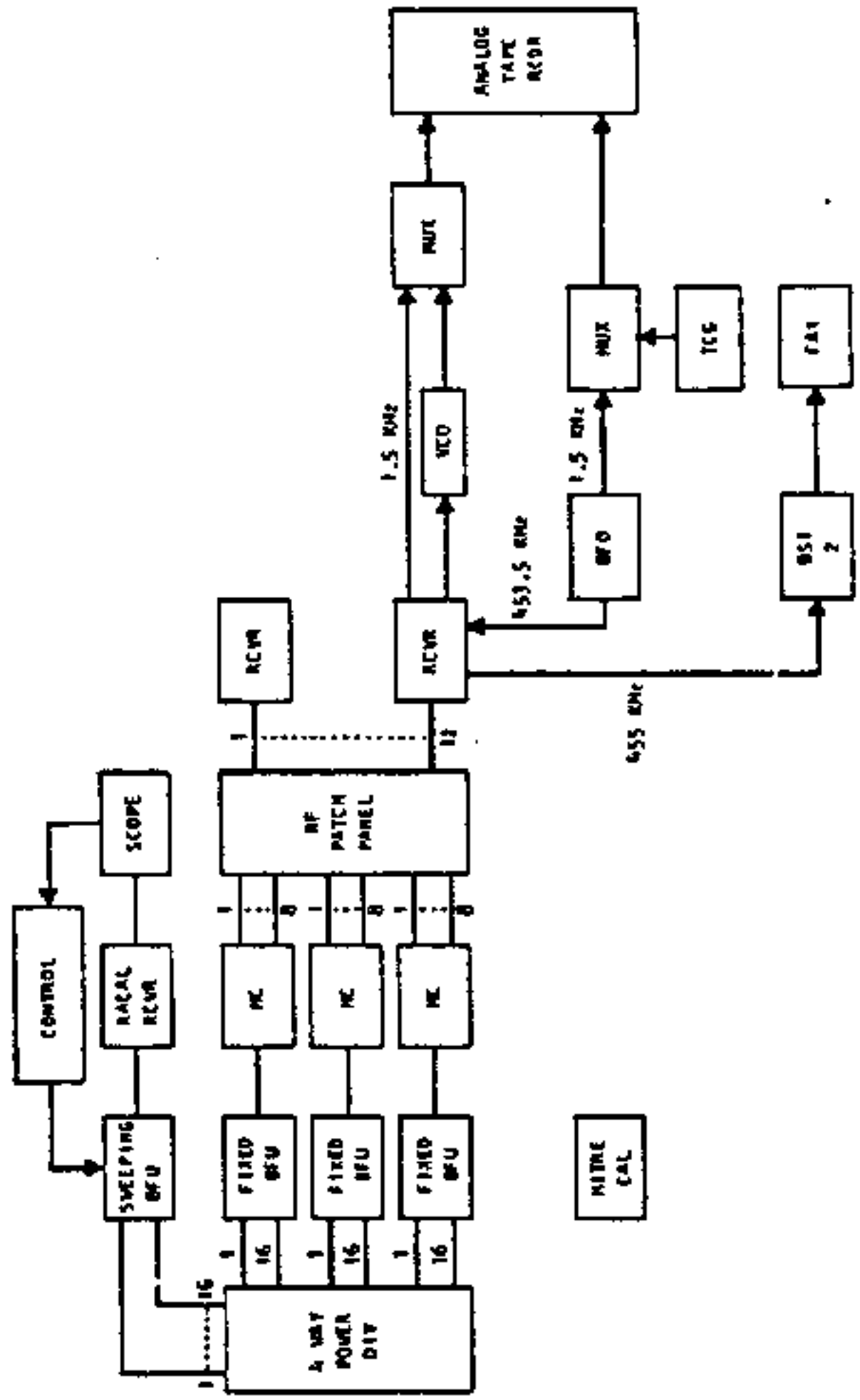

Figure 3. (U) Block Diagram of Twelve Channel Analog Receiving System (U).

2.3 (U) (S) -- Continued.

particular carrier signal is noted. Then the synthesizer at the same frequency is input to the antenna terminals and the output amplitude adjusted until the receiver IF output signal strength is the same. The synthesizer signal level is then measured, and converted to db with respect to a watt. Thus this signal substitution method gives the received carrier strength in dbw and is measured within the narrow IF receiver bandwidth.

The determination of the noise level at frequencies near the carrier is done by AM modulating the on-air carrier signal with an audio frequency square wave using a very small percentage modulation. The amplitude of these modulation tones is observed at the output of the real time spectrum analysis display. The modulation percentage is reduced until the modulation tones disappear into the background noise of the display. Since the modulation percentage is easily converted to signal level in db below the carrier and the spectrum analysis bandwidth is 1 Hz, then the relative carrier-to-noise power is directly obtained referenced to a 1 Hz bandwidth. Thus, if the calibration tone disappears into the noise at a level of 64 db below the carrier, it is assumed that the noise value is also 64 db below the carrier value. This carrier-to-noise ratio is then added to the received carrier strength to obtain the measured noise power in dbw per Hz.

2.4 (U) (S) Propagation Prediction.

The propagation prediction program used to estimate the system performance basically combines a modified version of the ITSA/ESSA HF propagation prediction program for mode and mode amplitude prediction; the bistatic radar range equation to predict the received scatter path power; and an ITSA/ESSA noise prediction program to estimate atmospheric, man made, and galactic noise at the receiver site.

SECRET

2.4 (U) -- Continued.

The prediction program package consists of individual computer programs that (a) compute a target trajectory; (b) predict propagation mode structure and mode amplitude; and (c) predict the Doppler and missile cross-section.

The trajectory simulation program estimates the missile or aircraft trajectory based upon fitting the flight profile to a functional form using a least-squares fit technique. The required inputs to generate the model profile are liftoff and burnout times, launch azimuth, apogee, and range. The program then computes altitude, range, latitude, longitude, velocity, the speed of sound, Mach number, Mach angle, local target bearings, local target elevation angles, and acceleration. The computed parameters serve as inputs to the propagation prediction program to determine mode structures with a time varying terminal point on the trajectory.

The ITSA/ESSA propagation prediction program has been modified to allow for non-congruent hop structures and for propagation to and reflection from a point above the earth. The program predicts the mode structures that meet ionospheric propagation conditions on each of the three paths: the direct path, the transmitter-target half path, and target-receiver half path. In addition, the propagation losses and antenna gains for each mode are determined. For each mode predicted on the transmitter-missile half path, an "incident" (at the target) elevation angle, measured from the local horizon, is found. For each mode predicted on the target-receiver half path, the "scattered" elevation angle is also found. These parameters are then used with a modeled profile to predict Doppler frequencies.

Propagation predictions are based on empirically derived world-wide numerical maps of vertical ionosonde data. The results are monthly ionospheric coefficients which can be used with the parabolic layer assumption (parabolic electron density variations in the E and F layers) to predict monthly average ionospheric conditions affecting a specific ray path at any hour of the day.

In the prediction model, all line of sight, E and F propagating modes are determined between the transmitter and the target, between the receiver and the target, and between the transmitter and the receiver. The determination of these "half paths" is a generalization of the ground-to-ground prediction technique to include the case of ground-to-elevation-point predictions.

After the mode structures that meet the ionospheric conditions are identified, (those between horizontal screening and ionospheric penetration) propagation losses and antenna gains are determined. The losses calculated are free space loss (inverse square law), D-layer absorption loss, and ground reflection loss. The NBS empirical adjustment factor is included on the direct-path predictions to account for non-calculated losses. This factor is statistical and varies with season, path length, and earth location of the path. No similar adjustment factor is used or known for the half paths. The antenna types are specified for the system and the appropriate gain routines or gain tables are used.

The target scattering model for missile targets above 100 km is a hyperboloid compressed-ambient ionization in the exhaust-plume bow shock wave. The shock-wave scattering surface is considered hyperboloidal from photographic observations which have shown that the shock-wave surface could be described by a second order function and that the shock-wave surface should be asymptotic to the Mach cone.

2.4 (B) -- Continued.

The direction of the rays for the transmitter-missile and receiver-missile propagation paths uniquely define a plane tangent to the hyperboloidal surface which has the proper orientation for a reflection, provided the incident ray encounters a high enough electron density for reflection.

Since little definitive work has been done to accurately model missile cross sections below 100 km or aircraft cross sections at HF, a constant (adjustable) cross section is used for aircraft and missile targets below 100 km.

The antenna gain patterns for both the monopole transmitter antennas and the LDAA receiving antenna are part of the program. The gain pattern for the LDAA was obtained from data supplied by ITT by using azimuth patterns predicted by the array factor technique for 16 monopole elements and the elevation patterns from scaled model measurements.

SECTION 3.

(U) (S) PREDICTED SYSTEM PERFORMANCE (U)

Propagation calculations to predict system performance using a modified version of the ESSA skywave propagation program described in the previous section have been made for both the direct and the scatter-paths between the receiver site at VHFS, and the buoy transmitters off the Florida coast. The purpose of these calculations was to estimate the feasibility of detecting SLBM missile launchings from Cape Kennedy and controlled aircraft targets using the geometry previously established of buoys at ranges of 100, 200 and 300 km from Cape Kennedy.

3.1 (U) (S) Missile Detection Performance.

Several sets of calculations using the computer predictions were performed. The receiving antenna at Vint Hill Farms Station used for all tests is a tulip element LDAA built by ITT with an assumed maximum gain of 16 dbi. A constant scattering cross section of 100 m^2 was assumed for the missile at all altitudes below 100 km. At altitudes above 100 km the bistatic cross section was modelled using a hyperboloid compressed ambient shock surface. The assumed cross section then changes from 10^2 m at low altitude to values of 10^4 to 10^5 m^2 above 100 km. The three buoy transmitter locations are at 100, 200 and 300 km directly down range from the 105° Cape Kennedy launch azimuth. The Carter Cay transmitters are approximately 285 km down range at a 123° azimuth from Cape Kennedy. The transmitted frequencies for the buoys were the presently assigned values of 5.8 and 9.295 MHz. These frequencies, plus frequencies of 15 and 20 MHz were assumed for the Carter Cay transmitters. The buoys were assumed to have

3.1 (U) (S) -- Continued.

a transmitting power of 100 watts radiating from monopole antennas. Similarly, the Carter Cay transmitters were assumed to be radiating 5 kw into monopole antennas.

Tables 1 through 5 summarize the results of the propagation calculations. Tables 1 through 4 show target signature-to-noise-ratio and carrier-to-signature ratio. Because of the low power and relatively low frequency from the buoy transmitters, the signal-to-noise ratio is almost always negligible below 100 km for any time of the day for either frequency. Only above 100 km with the enhanced target cross section does there appear to be any substantial chance of detection using the buoy transmitters. However, with the Carter Cay transmitter using 5 kw and transmitting on frequencies near the MUF as shown in Table 5 the signature-to-noise ratio and thus the probability of detection at even low altitudes is quite substantial. In fact, there are many cases for which the signal-to-noise ratio exceeds 15 db. Thus, if the high power Carter Cay transmitters continue to operate and transmit on frequencies near the 1 F hop MUF between Carter and VHFS then low altitude SLBM detections in the afternoon should be possible.

3.2 (U) (S) Aircraft Detection Areas.

Even though the probability of detecting SLBM launchings from Cape Kennedy is quite low (due to the relatively long range from the buoy to the target) it is important to determine whether or not aircraft flying controlled patterns near the buoys and Carter Cay can be detected. A way to evaluate this and to clearly display the results is to compute expected detection regions around the transmitter position. Variables that must be considered when calculating detectability regions are bistatic geometry, frequency, transmitter power, target cross section, skywave hop structure, sea state, local time of day and noise level. By choosing median values for

SECRET

Table I.

(U) Predicted System Performance for November, 1969

for Buoy 1 at 100 km Range from Cape Kennedy (U)

Altitude	Frequency (MHz)		00:00Z	04:00Z	08:00Z	12:00Z	16:00Z	20:00Z
5km	5.8	S/N	-3.6	-12.2	-14.4	-11.0	-42.6	-30.3
		PC/SB	80.5	80.5	81.3	82.1	83.5	82.6
	9259	S/N	-2.3	-8.8	-7.7	-3.4	-14.3	-5.0
		PC/SB	79.1	79.1	79.9	79.7	79.7	80.3
10km	5.8	S/N	-2.5	-12.1	-14.3	-11.0	-40.5	-31.2
		PC/SB	79.4	80.4	81.2	82.0	81.5	83.6
	9.259	S/N	-2.2	-8.7	-7.6	-3.3	-14.8	-5.0
		PC/SB	79.0	79.0	79.7	79.6	80.3	80.3
40km	5.8	S/N	-2.1	-11.5	-13.8	-10.7	-40.0	-31.9
		PC/SB	79.0	79.9	80.7	81.7	81.0	84.2
	9259	S/N	-0.6	-8.0	-6.9	-1.9	-18.5	-5.0
		PC/SB	77.4	78.4	79.1	78.2	83.9	80.2
119km	5.8	S/N	49.9	10.9	8.6	18.5	37.7	-1.8
		PC/SB	27.0	57.5	58.3	52.5	78.7	54.2
	9.259	S/N	41.5	2.8	3.89	48.1	23.0	24.6
		PC/SB	35.3	67.5	68.4	28.2	42.4	50.6

S/N = Target Signal-to-Noise Ratio (db)

PC/SB = Carrier-to-Target Signal Ratio (db)

Table 2.

(U) Predicted System Performance for November, 1967
for Buoy Z at 200 km Range from Cape Kennedy (U)

Altitude	Frequency (MHz)		00:00Z	04:00Z	08:00Z	12:00Z	16:00Z	20:00Z
5 km	9.259	S/N	-9.9	-18.5	-20.7	-17.3	-49.0	-36.5
	5.8	PC/SB	84.9	83.9	84.7	85.0	86.4	86.0
	9.259	S/N	-8.6	-15.1	-14.0	-9.7	-20.6	-11.3
	5.8	PC/SB	76.6	76.6	77.3	78.0	76.7	77.6
10 km	9.259	S/N	-8.9	-18.4	-20.7	-17.3	-46.9	-37.6
	5.8	PC/SB	93.9	83.9	84.7	85.0	84.4	87.0
	9.259	S/N	-8.5	-15.0	-13.9	-9.7	-21.2	-11.4
	5.8	PC/SB	76.5	76.5	77.2	77.9	77.3	77.6
40 km	9.259	S/N	-8.6	-18.1	-20.3	-17.2	-44.4	-33.5
	5.8	PC/SB	83.6	83.5	84.3	84.9	81.9	82.9
	9.259	S/N	-7.1	-14.5	-13.4	-8.4	-20.7	-11.5
	5.8	PC/SB	75.1	76.1	76.7	76.7	78.8	77.8
119 km	9.259	S/N	20.6	11.9	9.6	7.7	-49.1	-16.5
	5.8	PC/SB	54.4	53.6	54.4	60.0	86.6	68.0
	9.259	S/N	13.5	3.1	4.15	27.6	22.0	27.6
		PC/SB	54.7	58.5	59.2	40.6	34.1	38.6

S/N = Target Signal-to-Noise Ratio (db)

PC/SB = Carrier-to-Target Signal Ratio (db)

Table 3.

(U) Predicted System Performance for November, 19[illegible]
for Buoy 3 at 300 km Range from Cape Kennedy (U)

Skin Altitude	9.259 5.8 Frequency (MHz)		00:00Z	04:00Z	08:00Z	12:00Z	16:00Z	20:00Z
		S/N	-20.3	-30.4	-32.8	-28.3	-70.7	-55.2
		PC/SB	89.7	90.3	91.3	90.0	102.2	98.9
		S/N	-19.3				-34.9	-24.6
		PC/SB	78.4				82.0	82.2
	9.259 5.8	S/N	-12.5	-22.0	-24.3	-21.9	-50.5	-41.2
		PC/SB	81.9	81.9	82.8	82.7	82.0	85.0
10km	9.259 5.8	S/N	-12.2	-18.6	-17.5	-13.3	-24.8	-15.0
		PC/SB	71.2	71.2	72.3	72.9	82.5	72.6
	9.259 5.8	S/N	-12.4	-21.8	-24.1	-21.0	-48.1	-37.3
		PC/SB	81.8	81.7	82.5	82.7	79.7	81.0
10km	9.259 5.8	S/N	-10.9	-18.3	-17.2	-12.1	-23.9	-15.3
		PC/SB	70.0	70.9	72.0	71.7	71.[illegible]	70.9
	9.259 5.8	S/N	-10.0	2.3	-0.7	12.7	-50.9	-27.2
		PC/SB	59.5	57.6	59.1	49.0	86.4	70.6
119km	9.259 5.8	S/N	5.3	-4.3	-4.8	16.7	7.7	13.7
		PC/SB	55.7	56.9	59.6	42.9	39.4	43.9

S/N = Target Signal-to-Noise Ratio (db)

PC/SB = Carrier-to-Target Signal Ratio (db)

Table 4.

(U) Predicted System Performance for November, 1969.

for CARTER CAY Transmitters (U)

Altitude	Frequency (MHz)		00:00Z	04:00Z	08:00Z	12:00Z	16:00Z	20:00Z
5km	9.259	S/N	0.7	-7.8	-10.1	-6.7	-38.3	-25.9
		PC/SB	84.9	83.9	84.7	85.0	85.9	85.1
	5.8	S/N	2.1	-4.4	-3.3	0.9	-10.0	-0.7
		PC/SB	80.4	79.5	80.2	80.8	79.0	80.0
10km	9.259	S/N	1.8	-7.8	-10.0	-6.7	-36.2	-26.9
		PC/SB	83.5	83.9	84.7	85.0	83.9	86.1
	5.8	S/N	2.1	-4.3	-3.2	1.0	-10.5	-0.7
		PC/SB	80.3	79.4	80.1	80.8	79.6	80.1
40km	9.259	S/N	2.0	-7.5	-9.7	-6.6	-33.8	-22.9
		PC/SB	83.6	83.6	84.3	84.9	81.5	82.1
	5.8	S/N	3.5	-3.9	-2.8	2.2	-10.1	-0.9
		PC/SB	79.0	79.0	79.7	79.5	79.2	80.3
110km	9.259	S/N	36.8	27.3	24.8	21.5	-40.7	-10.4
		PC/SB	48.8	48.8	47.8	56.8	68.4	69.1
	5.8	S/N	29.2	21.0	20.1	45.2	24.7	25.3
		PC/SB	53.3	54.1	56.7	36.5	44.4	54.1

S/N = Target Signal-to-Noise Ratio (db)

PC/SB = Carrier-to-Target Signal Ratio (db)

TABLE 5.

(U) Predicted System Performance for November, 1969
for Carter Cay Transmitter Using Frequencies near the MUF. (U)

Altitude	Frequency		0000Z	MUF	0400	MUF	0800	MUF	1200	MUF	1600	MUF	2000	MUF
5 KM	15 MHz	S/N	9.93	13.56	-		-		-		13.4	21.80	10.4	21.07
		PC/SB	60.3		-		-		-		59.2		60.1	
	20 MHz	S/N	-		-		-		-		16.5	21.77	11.3	21.03
		PC/SB	-		-		-		-		73.3		74.8	
10 KM	15 MHz	S/N	10.0	13.65	-		-		-		12.3	22.07	10.4	21.28
		PC/SB	60.2		-		-		-		60.2		60.7	
	20 MHz	S/N	-		-		-		-		16.5	22.00	11.3	21.21
		PC/SB	-		-		-		-		73.4		74.8	
40 KM	15 MHz	S/N	11.3	14.20	-		-		19.3	12.99	12.0	23.73	9.2	22.60
		PC/SB	59.0		-		-		60.6		60.6		61.8	
	20 MHz	S/N	-		-		-		-		18.2	23.51	13.2	22.38
		PC/SB	-		-		-		-		71.7		72.9	
119 KM	15 MHz	S/N	26.7	15.83	-		-		47.1	14.70	33.5	14.53	51.1	26.40
		PC/SB	43.6		-		-		32.8		39.2		20.0	
	20 MHz	S/N	18.6	15.55	-		-		-		56.6	28.16	48.7	25.80
		PC/SB	190.4		-		-		-		33.2		37.4	

S/N = Target signal-to-noise ratio (db)

PC/SB = Carrier-to-target signal ratio (db)

3.2 (U) (S) -- Continued.

all the variables and changing the values of a single variable at a time, regions where detections are most likely to occur can be generated, as well as obtaining an understanding of how a particular variable affects the overall detection area.

Detectability regions have been calculated for various frequencies, hop structures and noise levels using a buoy located 120 km from Cape Kennedy as the transmitter and VIIFS, Va. as the receiver. A sea state of 5, transmitter power of 50 watts, groundwave propagation from transmitter to target and skywave propagation from target to receiver and a required signal to noise ratio of 3 db have been assumed.

The following technique is applied to find the area of detectability: From the radar range equation

$$L_R = L_{BT} + L_{BR} - G_T - G_R - \left[10 \log \frac{4\pi\sigma}{\lambda^2}\right]$$

where L_R = total loss
L_{BT} = spreading loss from transmitter to target (db)
L_{BR} = spreading loss from target to receiver (db)
G_T = gain of the transmitter antenna (dbi)
G_R = gain of the receiver antenna (dbi)
σ = cross section of target in m^2
λ = wave length

G_T, G_R and $10 \log \frac{4\pi\sigma}{\lambda^2}$ are known and L_R is calculated by assuming a value for atmospheric noise, adding to it the transmitter power and the required 3 db signal-to-noise ratio. Substituting the calculated value for

3.2 (U) (S) -- Continued.

L_R into the equation, $L_{BT} + L_{BR}$ is calculated. By taking the total spreading loss, subtracting the loss contributed by the D layer loss and skywave propagation loss from target to receiver, a value for the spreading loss in the target-transmitter leg is obtained. This loss is the propagation loss incurred by a groundwave and can be converted to the range required for this loss to occur using Barrick's[1] groundwave transmission loss tables. This technique was used to calculate the detection area around the transmitter for various frequencies and atmospheric noise conditions. The results of the detection area calculations are tabulated in Table 6 and a vertical projection of some of the regions onto the ground is shown in Figure 4. The reason for the egg-like shape is that the area boundary is the locus of points such that the product $R_1 R_2$ is equal to a constant.

Referring to Figure 4 we see that the largest area of detection is for 2F hop cases for both 5.8 and 9.259 MHz, as compared to the 1E hop situation. This is because there is substantially less D-layer loss for the 2F hop mode than the 1E hop mode due primarily to the different path lengths in the D-region itself. With higher modes the incident angle through the D-layer is higher, thus the loss on these paths due to D-layer absorption is smaller. For the 2F hop modes the region at 5.8 MHz is larger than the region at 9.259 MHz. This is due to the fact that the loss on the R1 path is smaller at lower frequencies because the spreading loss is directly proportional to the wavelength and as one would expect the larger region for detection exists for the lower frequency. However, on the 1E modes we find the situation is reversed, the higher frequency is also the larger area of detection. This is because the D-layer loss on the 5.8 MHz frequency is substantially more than the D-layer loss at 9.259 MHz and this overcomes the groundwave propagation advantage at the lower frequency.

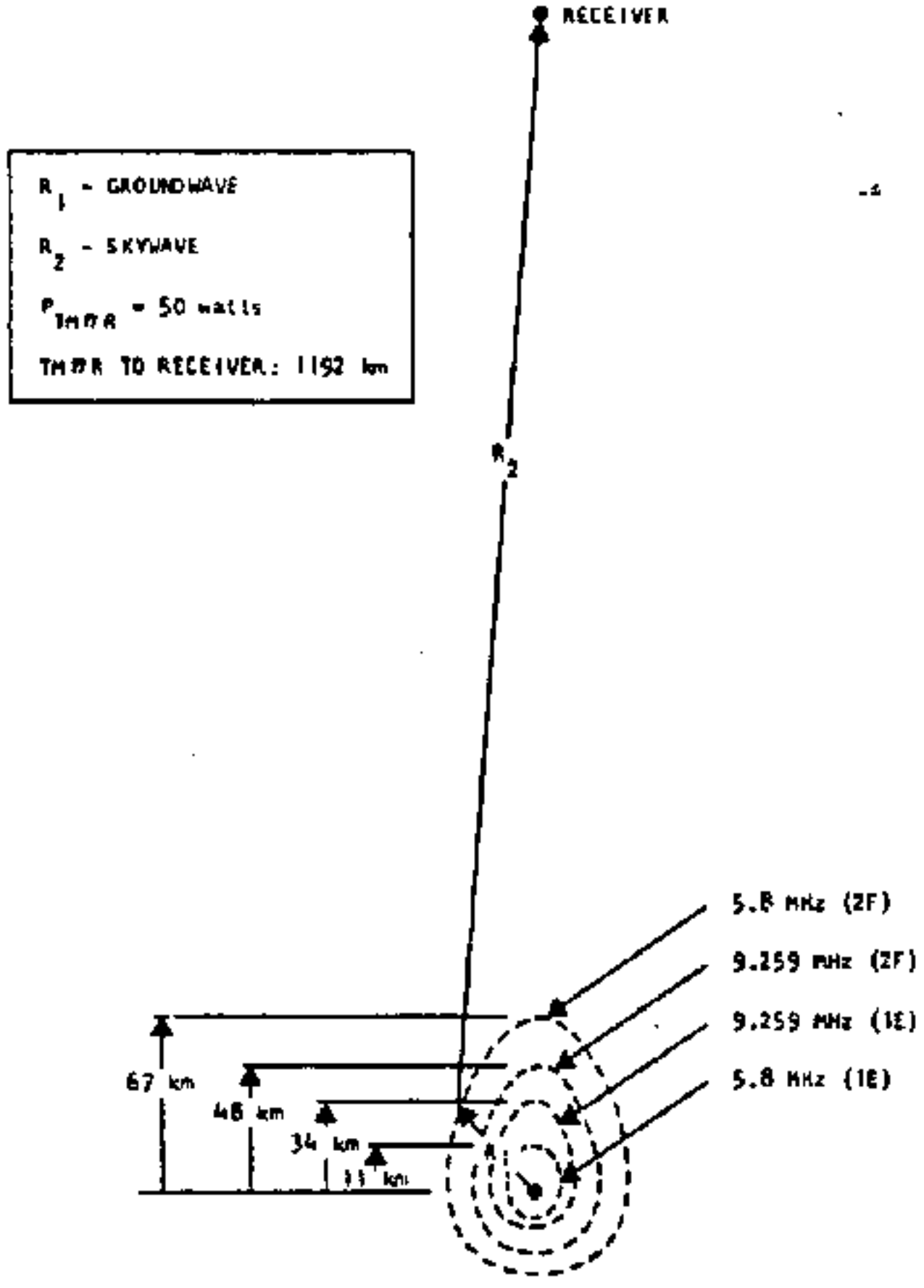

Figure 4. (U) Sample Detection Regions (U).

Table 6.

(U) Summary of Detection Region Calculations (U)

Freq MHz	Hop Structure	R_1 Km	R_1 Loss db	$L_{BT}+L_{BR}$ Loss db	D-Layer Loss db	R_2 Loss db	Atmos Noise dbw
5.8	1E	11	61	211.7	48.5	102.2	-180(B)
5.8	2F	67	79.1	211.7	30.4	102.2	-180(B)
5.8	1E	10	59.5	195.7	34	102.2	-153(M)
9.259	1E	34	80.1	210.7	21.9	108.7	-172(B)
9.259	2F	48	86.2	210.7	15.8	108.7	-172(B)
9.259	1E	64	84.7	208.7	15.3	108.7	-169(M)
9.259	1F	65	90.8	208.7	9.2	108.7	-169(M)
15.00	1F	60	101	216.9	4.0	112	-174(M)
15.00	1F	67	103.6	221.5	5.9	112	-176(B)
20.0	1F	66	113.9	231.5	3.1	114.5	-186(B)
20.0	1F	66	113.6	230.1	2.1	114.5	-185(M)

B = Best noise case 0800-1200 Local Time

M = Medium noise case 1600-1200 Local Time

From Table 6 we see that the detectability radii (R_1) tend to increase with increasing transmitted frequency. However, once the frequency increases to approximately 15 MHz, the R_1 spreading losses cancel the effect of decreasing D-layer loss and decreasing atmospheric noise so that the growth of the detectability region virtually stops. Note that the detectable radii are approximately the same for 15 and 20 MHz. It is also observed that varying transmitter power and tranamitter or receiver antenna gains have the same effect on the size of the detectability regions. That is a db of gain or loss whether generated from varying transmitter power or antenna gain enters the radar range equation in the same way.

SECTION 4.

(U) (S) DATA ANALYSIS (U)

In this section, two events involving a controlled aircraft flight of a Navy P3B aircraft and two propagation measurements between Carter Cay and VHFS are presented with their specific geometry, predicted and measured results and conclusions derived from the results. These operations are summarized in Table 7 and a map of the network geometry is shown in Figure 5.

4.1 (U) (S) Event 1.

Event 1 on 18 December, 1969, involved a Navy P3B aircraft flying at an altitude between 300 to 600 feet, speed between 200 and 400 knots and used the buoy transmitter located 120 km from Cape Kennedy on an azimuth of 113°. The flight path of the aircraft, along with time (GMT) is shown in Figure 6. The receiver location for this event, as with all Aquarius events, was VHFS, Virginia. The two buoy frequencies of 5.8 and 9.259 MHz were monitored by the receiver. A signature detection was made on 5.8 MHz between 1750-1755Z and 2000Z-2005Z. The propagation conditions are summarized below:

Table 7 (U)
Event 1 Summary (U)

Frequency (MHz)	Carrier Level (dbw)	Noise Level (dbw)	Transmitter Power (W)	Calculated Detection Radii (km)	Hop Structure
5.8	-92	-160	10	3	1E
				6	2F
9.259	-130	-157	2.5	11	1F
				6	1E

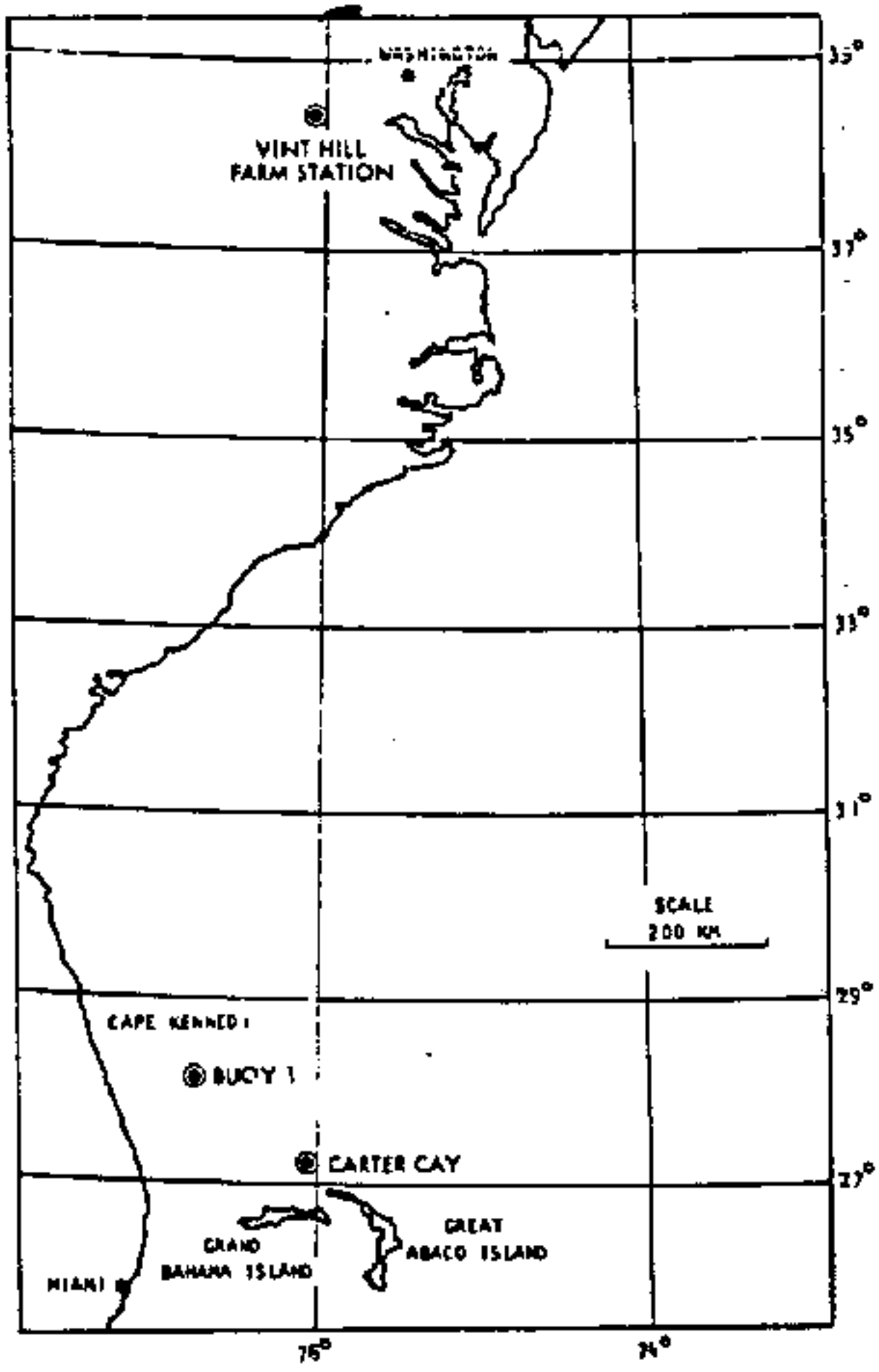

Figure 5. (U) Network Geometry (U).

Table 8.

(U) Summary of Operations (U)

EVENT	DATE	TYPE	FREQUENCIES (MHz)	MEASUREMENT OR DETECTION TIMES (GMT)
1	18 Dec 69	AC	5.8	1750-1755 2000-2005
		AC	9.259	ND
		AC	10.167	ND
2	27 Jan 70	AC	15.595	1656
3	27 Jan 70	AC	10.167	1712
4	5 Feb 70	HB	20.250	~1500
		HB	10.167	~1500
		HB	10.167	~2100
		HB	20.250	~2100
5	10 Feb 70	HB	9.259	~1430
		HB	5.8	~1430

AC - Aircraft

ND - Not Detected

HB - Hearability

4.1 (U) (S) -- Continued.

It is felt that the detected signature is not the Navy P3B aircraft used in this test but on aircraft flying near the receiver at VHFS. The predicted detectability region for this day extends at best to only 31 km. The P3B aircraft approaches the buoy within only 30 km. The period of the first Doppler signature's sign change occurs 5.2 minutes later than predicted closest approach and the period of the second Doppler signature sign change occurs 2.8 minutes earlier than predicted closest approach. The Doppler signatures obtained shown in Figures 7 and 8 were of the proper frequency for an aircraft but were much stronger than could be expected from a 10 watt transmitter. Thus, due to inconsistant timing, distances of aircraft from the transmitter, strength of detected signatures, and the low power of the transmitters, it is concluded that signature detected was not the P3B aircraft used in the experiment but rather another plane flying over the receiving antenna.

4.2 (U) (S) Events 2 and 3.

Events 2 and 3 on January 27, 1970 involved an aircraft (P3B) climbing to an initial altitude of 24,000 feet and spiralling down to 2000 feet while holding a precise test pattern and maintaining ground speed between 200-300 knots. The aircraft flew the pattern described by Figure 10. Initially approaching the Carter Cay area on its way from CP C3 to CP C8, the aircraft proceeded to fly the pattern C8 to C7 to C6 to Carter Cay to D4 to D5 to Carter Cay to C5 and repeating for altitudes of 24,000, 14,000, 12,000 and 2000 feet. The transmitters were again located on Carter Cay. The frequencies monitored by the receiver at Vint Hill Farms Station were 10.167 and 15.598 MHz. Detection was made at 1712Z on 10.167 MHz and

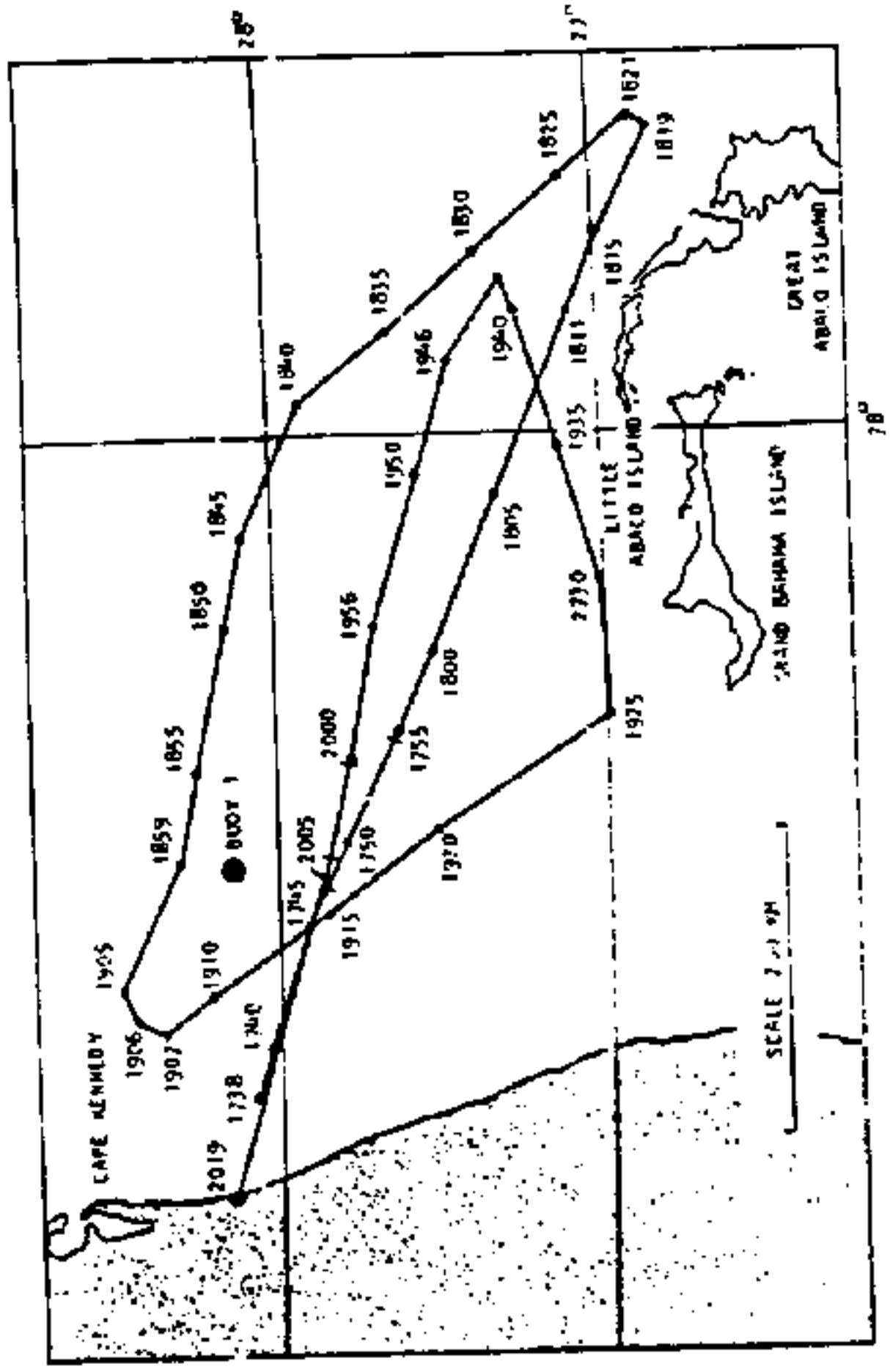

Figure 6. (U) Event I Flight Pattern (U).

UNCLASSIFIED

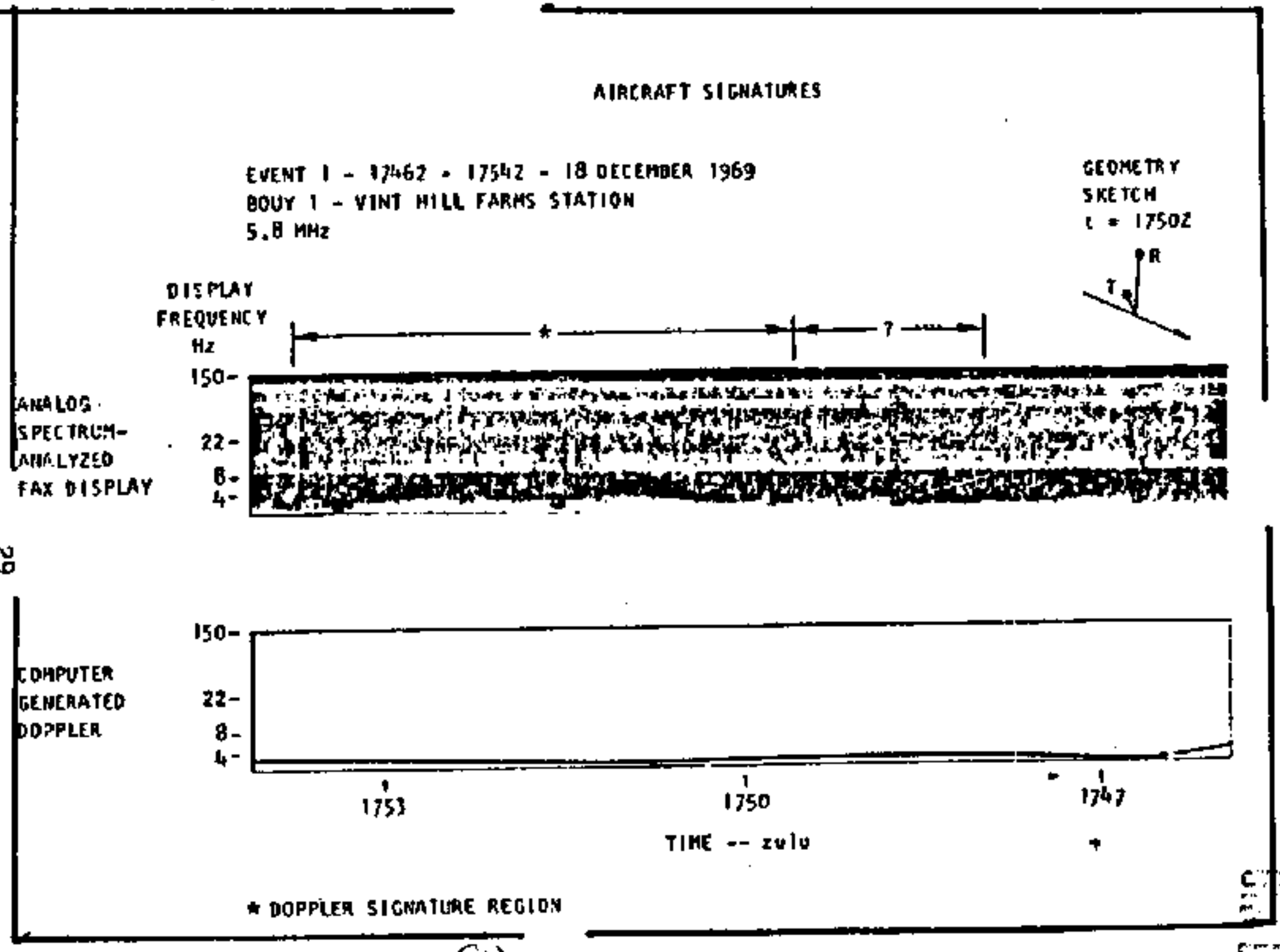

(U)

Figure 7. (~~SECRET~~). Experimentally Collected Data (U).

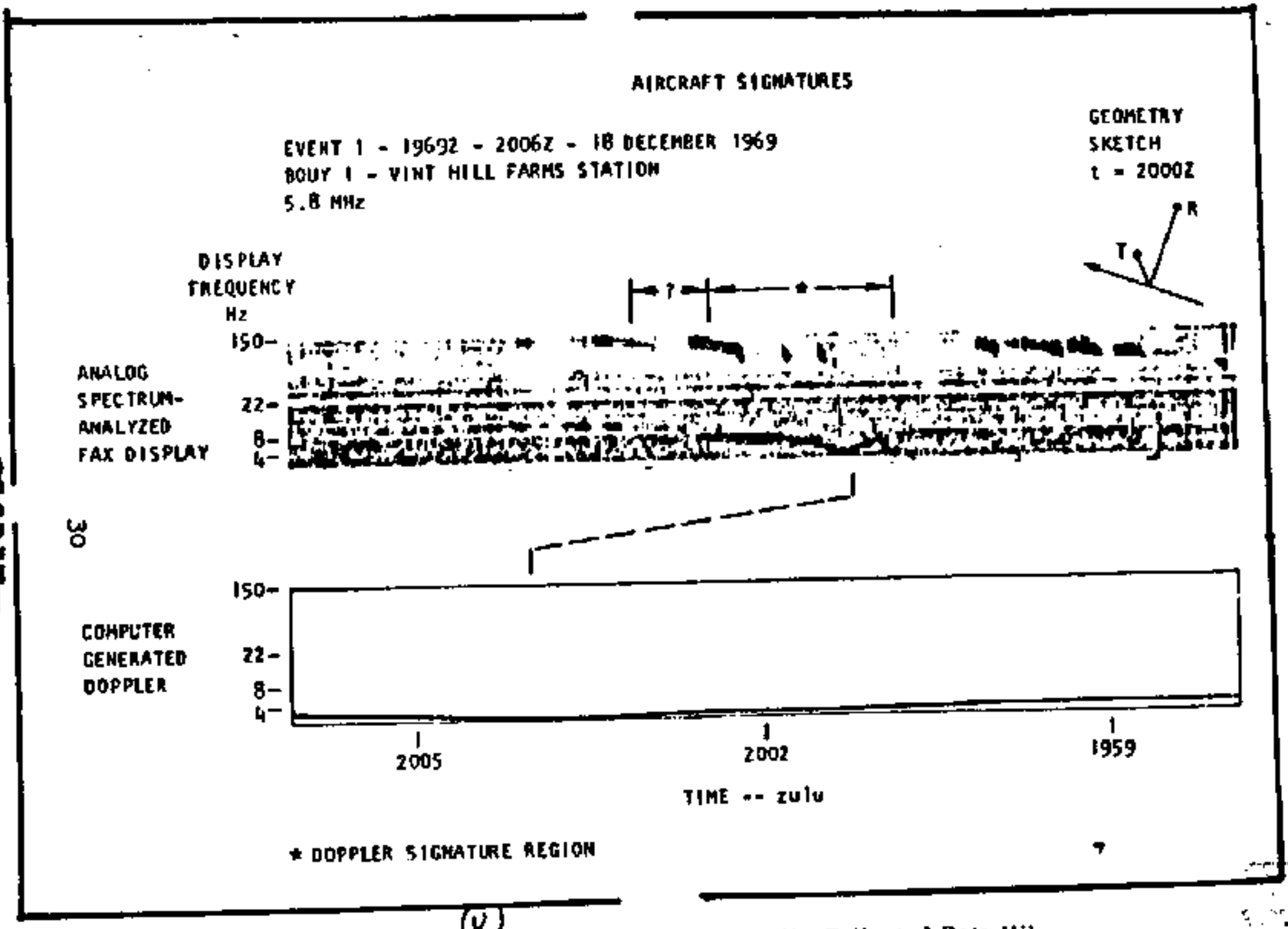

Figure 8. (U) (~~SECRET~~). Experimentally Collected Data (U).

4.2 (U) -- Continued.

at 15.595 MHz as shown on Figure 9. The propagation conditions for these events are summarized below:

Table 9. (U)

Event 2 and 3 Summary

Frequency (MHz)	Carrier Level (dbw)	Noise Level (dbw)	Tx Power (w)	Detection Time (Z)
10.167	-112	NA	3000	1712
15.595	NA	-145	3000	1655

The signatures detected on this event represent the scattered and doppler shifted energy from the target aircraft during the time of close approach to Carter Cay. However, accurate doppler predictions have not yet been made due to the inexact knowledge of the flight path and the fact that the detections appear to be made during the end of the turning maneuver over Carter. The present doppler modelling for aircraft is being modified to handle out of plane maneuvers and from this improved model, accurate doppler matches will be possible.

We observe from Figure 10 that the detections for both passes on Carter were slightly late with respect to the time that the aircraft indicates it was directly over the transmitter. There is a good possibility that the aircraft flew exactly over the transmitting antenna and thus was in the vertical pattern antenna null. Being in the null of the antenna explains the loss of signature for times over the transmitter. The signatures are detected at the completions of the turning maneuvers over Carter Cay. Signatures for both detected passes of the aircraft are almost identical in both timing and frequency. Thus, the frequency excursion, time correlation, nearness of the aircraft to the transmitter, radiated power from the Carter Cay transmitters, and the weak signature strength make the

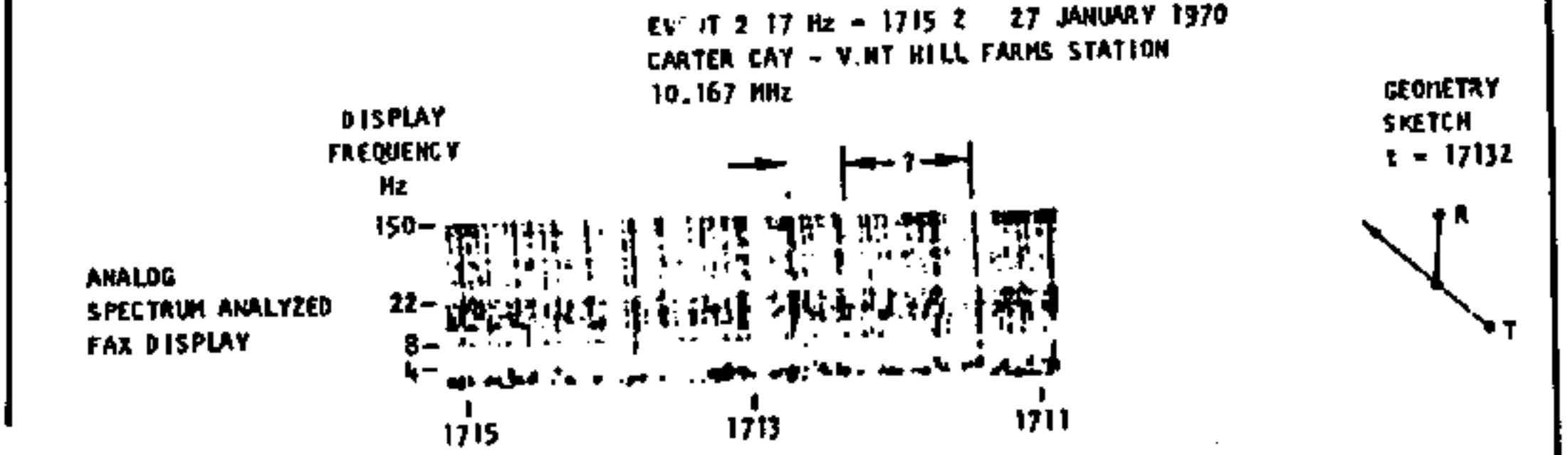

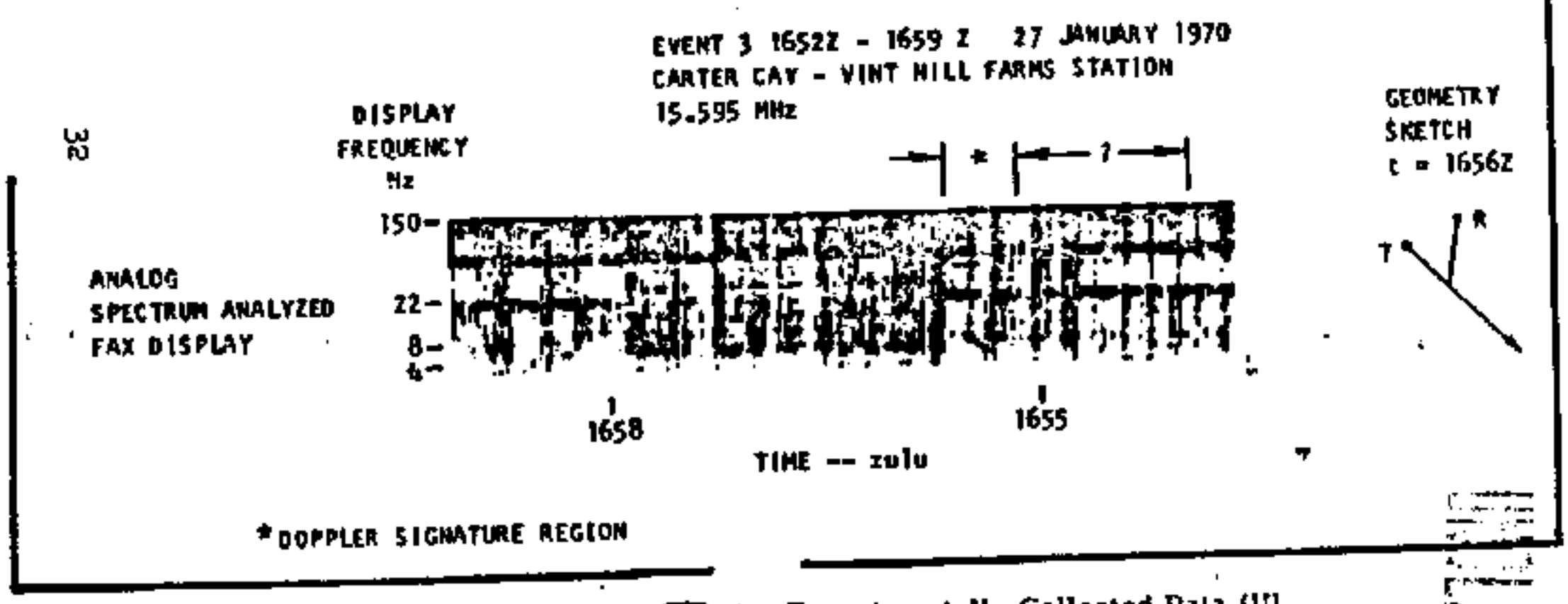

Figure 9. (~~CORRECTED~~) Experimentally Collected Data (U).

(U)

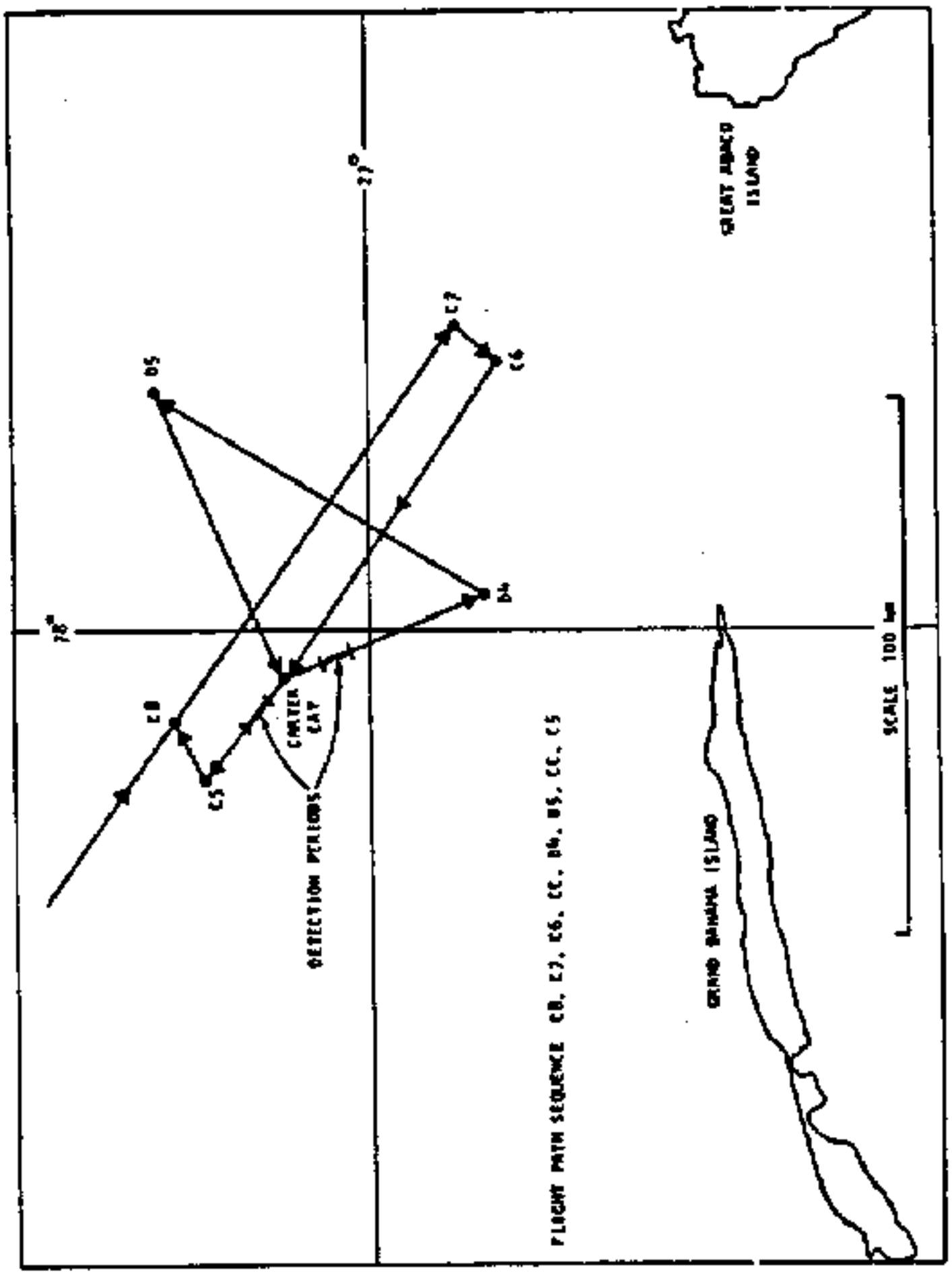

Figure 10. (U) Flight Path for Events 2 and 3 (U).

(U)

4.2 (S) -- Continued.

identification of the signature as the target PJD aircraft. The conclusion is that aircraft below 2K feet and within the predicted detectability regions can be detected using this buoy concept if sufficient power is transmitted (3 kw in this case).

4.3 (U) Event 4.

Event 4 was a hearability test, performed on 5 February at 1600 and 1000 hours local, measuring the propagation characteristics from Carter Cay transmitters to the Vint Hill Farms Station receiver. The purpose of the hearability test was to determine how accurately present prediction techniques correlate with measured values and to estimate the hop structures for various frequencies. Tests were performed for two frequencies 10.167 and 20.250 MHz and at two times during the day. It was found that for an assumed 1E hop structure at 10.167 MHz and an assumed 1F hop structure at 20.250 MHz good agreement between predicted and observed carrier levels was obtained. However, the noise predictions were consistently lower than measured values as shown in Table 10. The difference between the predicted and observed noise levels is typically due to co-channel interference which is significantly higher than atmospheric noise.

Table 10 (U)

Comparison of Predicted and Observed Carrier and Noise Levels (U)

Date/Time	Frequency (MHz)	Assumed Hop Structure	Tx Power (kw)	Carrier (dbw) Pred.	Carrier (dbw) Obs.	Noise (dbw) Pred.	Noise (dbw) Obs.
Feb 1600L	10.467	1E	2.1	-79	-76	-162.8	-144
Feb 1000L	10.167	1F	2.1	-58.9	-90	-163	-158
Feb 1600L	20.250	1F	2.1	-62.7	-66	-179.1	-134

4.4 (U) Event 5.

Event 5 was also a hearability test, performed on 16 Feb. at 1430 local time, with the same geometry and purpose as Event 4. Tests were performed for 5.8 and 9.259 MHz. As shown in Table 11, best correlation between measured and observed carrier levels was obtained for an assumed 2F hop structure at 5.8 MHz and an assumed 1E hop structure at 9.259 MHz. As in Event 4, the noise predictions were consistantly lower than measured values. The conclusions from Events 4 and 5 is that 1E, 1F and 2F appear to be the dominate hop structures for 10, 20, 5 MHz respectively. It is also concluded from this limited data base that the propagation prediction is fairly accurate for predicting the received carrier levels, but due to high co-channel interference consistently predicts lower noise levels than are measured.

Table 11.

Comparison of Predicted and Observed Carrier and Noise Levels (U)

Date/Time	Frequency (MHz)	Assumed Hop	Transmitter Power	Carrier (dbw) Pred.	Carrier (dbw) Obs.	Noise (dbw) Pred.	Noise (dbw) Obs.
Feb. 1430L	5.8	1E	75w	-128.2	-110	-160.3	-160
Feb. 1430L		2F	75w	-124.6	110	-162.3	-160
Feb. 1430L	9.259	1E	75w	- 93.2	- 95	-162.8	-139
Feb. 1430L		2F	75w	-104	- 95	-162.8	-139

Section 5.

(U) (S) SUMMARY (U)

The operations covered to date include both controlled aircraft tests and hearability tests. The remainder of the operations have not been analyzed because all data on the events including flight paths and transmitter power have not yet been collected at Sylvania for analysis. The most significant conclusion is from Event 2 which seems to demonstrate that the buoy transmitter concept works (with sufficient transmitter power).

The predictions of carrier levels made for the hearability tests on 5 February and 11 February seem to align rather well with measured values. Predictions of noise level is not as successful, being consistently weaker than measured values. This is probably due to local interference and the assumption that the receiving site at VHFS is a "rural" man-made radio noise area. Identification of the receiver site as a "suburban" area is probably more accurate. This would raise the predicted noise level by approximately 20 db thus making it align with measured values much more closely.

SECTION 6.

REFERENCES

1. Banich, Donald E., "Theory of Ground-Wave Propagation Across a Rough Sea at HF/VHF", Battelle Memorial Institute, Draft Report.

END

DATE FILMED

4-70